Journal of Asian Earth Sciences 36 (2009) 74–83

Contents lists available at ScienceDirect

Journal of Asian Earth Sciences

journal homepage: www.elsevier.com/locate/jaes

Simulation of Andaman 2004 tsunami for assessing impact on Malaysia

Hock Lye Koh [a,*], Su Yean Teh [a], Philip Li–Fan Liu [b], Ahmad Izani Md. Ismail [a], Hooi Ling Lee [c]

[a] School of Mathematical Sciences, Universiti Sains Malaysia, 11800 Penang, Malaysia
[b] School of Civil and Environmental Engineering, Cornell University, USA
[c] Technip GeoProduction (M) Sdn Bhd, Kuala Lumpur, Malaysia

ARTICLE INFO

Article history:
Received 27 April 2008
Received in revised form 5 September 2008
Accepted 17 September 2008

Keywords:
Andaman tsunami simulation
TUNA
COMCOT
Malaysia

ABSTRACT

Mistakenly perceived as safe from the hazards of tsunami, Malaysia faced a rude awakening by the 26 December 2004 Andaman tsunami. Since the event, Malaysia has started active research on some aspects of tsunami, including numerical simulations of tsunami and the role of mangrove as a mitigation measure against tsunami hazards. An in-house tsunami numerical simulation model TUNA has been developed and applied to the 26 December 2004 Andaman tsunami to simulate the generation, propagation and inundation processes along affected beaches in Malaysia. Mildly nonlinear bottom friction term in the deeper ocean is excluded, as it is insignificant to the simulation results, consistent with theoretical expectation. On the other hand, in regions with shallow depth near the beaches, friction and nonlinearity are significant and are included in TUNA. Simulation results with TUNA indicate satisfactory performance when compared with COMCOT and on-site survey results.

1. Introduction

An earthquake at the Richter scale of 9.3 occurred on 26 December 2004 near northwest coast of Aceh Indonesia. This earthquake triggered a series of large tsunamis that killed around 250, 000 people in the affected areas, including 68 deaths in Malaysia. The needs for community education, preparedness and mitigation to face potential tsunami attacks among the coastal communities in Malaysia have been highlighted since the occurrence of the Andaman tsunami. The ability to simulate the generation, propagation and beach runup of tsunami is an essential component in the development of local capability to enhance community preparedness to mitigate the hazards of future tsunamis.

The evolution of earthquake-generated tsunami waves has three distinct stages: generation, propagation and runup. Two types of source generation terms are evaluated in this paper. The first is a simple Gaussian hump in the shape of an elongated ellipse (Yoon, 2002), while the second source term is based upon a model proposed by Okada (1985). Both source terms are generated with inputs derived from extensive literature review relating to the tsunami. The depth-averaged two-dimensional shallow water equations (SWE) are used to simulate the subsequent propagation of tsunami away from the source through the deep ocean. These models follow guidelines stipulated by the UNESCO intergovernmental oceanography commission (IOC, 1997). The SWE is used to simulate the propagation of tsunami waves across the deep ocean from the source of generation to offshore regions up to the depth of about 50 m in the Malaysia coasts. Using wave velocities and heights recorded at these offshore locations, a nonlinear shallow water equation model NSWE is then used to simulate the runup of tsunami waves onto the shallow beaches. The SWE is simulated by means of the in-house model TUNA-M2, while simulation of the beach runup is performed by the model TUNA-RP.

2. Shallow water equations

The propagation of tsunami across deep oceans may be simulated by the depth-averaged two-dimensional SWE as proposed by the intergovernmental oceanography commission. The SWE is applicable when the wave heights are much smaller than the depths of water, which in turn are much smaller than the wavelengths. Depth-averaged two-dimensional models are normally used for tsunami propagation simulations, as these models provide adequate solution. On the other hand, three-dimensional models would require excessive memory and long computational time, and hence are rarely used. Hence, under normal assumptions typically applicable to tsunami propagations in the deep ocean, the hydrodynamic equations describing the conservation of mass and momentum can be depth-averaged in two-dimensional forms (Hérbert et al., 2005; IOC, 1997) and may be written as Eqs. (1)–(3).

$$\frac{\partial \eta}{\partial t} + \frac{\partial M}{\partial x} + \frac{\partial N}{\partial y} = 0 \tag{1}$$

* Corresponding author. Tel.: +604 6533657; fax: +604 6570910.
E-mail address: hlkoh@cs.usm.my (H.L. Koh).

1367-9120/$ - see front matter © 2008 Elsevier Ltd. All rights reserved.
doi:10.1016/j.jseaes.2008.09.008

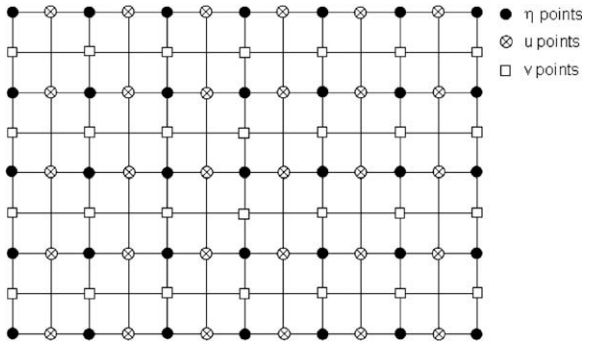

Fig. 1. Computational points for a staggered scheme.

$$\frac{\partial M}{\partial t}+\frac{\partial}{\partial x}\left(\frac{M^2}{D}\right)+\frac{\partial}{\partial y}\left(\frac{MN}{D}\right)+gD\frac{\partial \eta}{\partial x}+\frac{gn^2}{D^{7/3}}M\sqrt{M^2+N^2}=0 \qquad (2)$$

$$\frac{\partial N}{\partial t}+\frac{\partial}{\partial x}\left(\frac{MN}{D}\right)+\frac{\partial}{\partial y}\left(\frac{N^2}{D}\right)+gD\frac{\partial \eta}{\partial y}+\frac{gn^2}{D^{7/3}}N\sqrt{M^2+N^2}=0 \qquad (3)$$

Here, discharge fluxes (M, N) in the x- and y- directions are related to velocities u and v by the expressions $M = u(h + \eta) = uD$, $N = v(h + \eta) = vD$. Further D is the total water depth, h is the mean sea depth, and η is the instantaneous water elevation above mean sea level, g (9.81 m/s^2) is gravitational acceleration and n Manning friction coefficient. The shallow water equation can be solved by several methods, such as the finite element method and finite difference method. The explicit staggered finite difference method will be employed in this paper, as it is known to perform well, provided that Δt fulfils the Courant stability criterion. The finite difference method is also employed by many well-known models, such as COMCOT (Liu et al., 1998), TUNAMI-N2 (Imamura et al., 1988) and MOST (Titov and Synolakis, 1997). The explicit staggered finite difference scheme used in this paper is shown schematically in Fig. 1, while the mathematical formulation is indicated in Eq. (4), subject to the Courant stability criterion Eq. (5). It should be noted that the mildly nonlinear bottom friction terms and advection terms not represented in Eq. (4) are written separately in Eq. (6) for convenience of expression.

$$\begin{aligned}
\eta_{i,j}^{k+1} &= \eta_{i,j}^{k}-\frac{\Delta t}{\Delta x}\left[M_{i+0.5,j}^{k+0.5}-M_{i-0.5,j}^{k+0.5}\right]-\frac{\Delta t}{\Delta y}\left[N_{i,j+0.5}^{k+0.5}-N_{i,j-0.5}^{k+0.5}\right]\\
M_{i+0.5,j}^{k+0.5} &= M_{i+0.5,j}^{k-0.5}-gD_{i+0.5,j}^{k}\frac{\Delta t}{\Delta x}\left[\eta_{i+1,j}^{k}-\eta_{i,j}^{k}\right]\\
D_{i+0.5,j}^{k} &= h_{i+0.5,j}+0.5\left[\eta_{i+1,j}^{k}+\eta_{i,j}^{k}\right]\\
N_{i,j+0.5}^{k+0.5} &= N_{i,j+0.5}^{k-0.5}-gD_{i,j+0.5}^{k}\frac{\Delta t}{\Delta y}\left[\eta_{i,j+1}^{k}-\eta_{i,j}^{k}\right]\\
D_{i,j+0.5}^{k} &= h_{i,j+0.5}+0.5\left[\eta_{i,j+1}^{k}+\eta_{i,j}^{k}\right]
\end{aligned} \qquad (4)$$

$$\Delta t \leqslant \frac{\Delta x}{\sqrt{2gh}} \qquad (5)$$

The complicated discretization of the nonlinear bottom friction and advection terms is shown separately in Eq. (6), as adopted from IOC (1997). These nonlinear terms are incorporated into TUNA with an option of bypass.

$$\begin{aligned}
\frac{\partial}{\partial x}\left(\frac{M^2}{D}\right) &= \frac{1}{\Delta x}\left[\lambda_{11}\frac{\left(M_{i+1.5,j}^{k-0.5}\right)^2}{D_{i+1.5,j}^{k-0.5}}+\lambda_{21}\frac{\left(M_{i+0.5,j}^{k-0.5}\right)^2}{D_{i+0.5,j}^{k-0.5}}+\lambda_{31}\frac{\left(M_{i-0.5,j}^{k-0.5}\right)^2}{D_{i-0.5,j}^{k-0.5}}\right]\\
\frac{\partial}{\partial y}\left(\frac{N^2}{D}\right) &= \frac{1}{\Delta y}\left[\gamma_{12}\frac{\left(N_{i,j+1.5}^{k-0.5}\right)^2}{D_{i,j+1.5}^{k-0.5}}+\gamma_{22}\frac{\left(N_{i,j+0.5}^{k-0.5}\right)^2}{D_{i,j+0.5}^{k-0.5}}+\gamma_{32}\frac{\left(N_{i,j-0.5}^{k-0.5}\right)^2}{D_{i,j-0.5}^{k-0.5}}\right]\\
\frac{\partial}{\partial y}\left(\frac{MN}{D}\right) &= \frac{1}{\Delta y}\left[\gamma_{11}\frac{M_{i+0.5,j+1}^{k-0.5}N_{i+0.5,j+1}^{k-0.5}}{D_{i+0.5,j+1}^{k-0.5}}+\gamma_{21}\frac{M_{i+0.5,j}^{k-0.5}N_{i+0.5,j}^{k-0.5}}{D_{i+0.5,j}^{k-0.5}}+\gamma_{31}\frac{M_{i+0.5,j-1}^{k-0.5}N_{i+0.5,j-1}^{k-0.5}}{D_{i+0.5,j-1}^{k-0.5}}\right]\\
\frac{\partial}{\partial x}\left(\frac{MN}{D}\right) &= \frac{1}{\Delta x}\left[\lambda_{12}\frac{M_{i+1,j+0.5}^{k-0.5}N_{i+1,j+0.5}^{k-0.5}}{D_{i+1,j+0.5}^{k-0.5}}+\lambda_{22}\frac{M_{i,j+0.5}^{k-0.5}N_{i,j+0.5}^{k-0.5}}{D_{i,j+0.5}^{k-0.5}}+\lambda_{32}\frac{M_{i-1,j+0.5}^{k-0.5}N_{i-1,j+0.5}^{k-0.5}}{D_{i-1,j+0.5}^{k-0.5}}\right]\\
M_{i+0.5,j}^{k-0.5} &\geqslant 0, \lambda_{11}=0, \lambda_{21}=1, \lambda_{31}=-1 \quad 0, \lambda_{11}=1, \lambda_{21}=-1, \lambda_{31}=0\\
N_{i+0.5,j}^{k-0.5} &\geqslant 0, \gamma_{11}=0, \gamma_{21}=1, \gamma_{31}=-1 \quad 0, \gamma_{11}=1, \gamma_{21}=-1, \gamma_{31}=0\\
M_{i,j+0.5}^{k-0.5} &\geqslant 0, \lambda_{12}=0, \lambda_{22}=1, \lambda_{32}=-1 \quad 0, \lambda_{11}2=1, \lambda_{22}=-1, \lambda_{32}=0\\
N_{i,j+0.5}^{k-0.5} &\geqslant 0, \gamma_{12}=0, \gamma_{22}=1, \gamma_{32}=-1 \quad 0, \gamma_{12}=1, \gamma_{22}=-1, \gamma_{32}=0\\
\frac{gn^2}{D^{7/3}}M\sqrt{M^2+N^2} &= \frac{gn^2}{\left(D_{i+0.5,j}^{k-0.5}\right)^{7/3}}\times 0.5\left[M_{i+0.5,j}^{k+0.5}+M_{i+0.5,j}^{k-0.5}\right]\sqrt{\left(M_{i+0.5,j}^{k-0.5}\right)^2+\left(N_{i+0.5,j}^{k-0.5}\right)^2}\\
\frac{gn^2}{D^{7/3}}N\sqrt{M^2+N^2} &= \frac{gn^2}{\left(D_{i,j+0.5}^{k-0.5}\right)^{7/3}}\times 0.5\left[N_{i,j+0.5}^{k+0.5}+N_{i,j+0.5}^{k-0.5}\right]\sqrt{\left(M_{i,j+0.5}^{k-0.5}\right)^2+\left(N_{i,j+0.5}^{k-0.5}\right)^2}
\end{aligned} \qquad (6)$$

3. Comparing TUNA and COMCOT

An in-house tsunami simulation model TUNA is developed based upon the explicit finite difference method described above.

The simulation results of TUNA have been verified by comparing them with known analytical solutions in rectangular domains (Koh, 2007; 2005; Teh et al., 2006). In this paper we further extend the verification by comparing simulation results with those derived from COMCOT (Cornell Multi-grid Coupled Tsunami Model), the results of which indicate satisfactory performance of TUNA. A computational domain in the form of a channel of dimension 10 km by 40 km with a depth of 10 m is chosen for this comparison study. Solid boundary condition is imposed at the north, south and west ends of the channel to simulate complete reflection of waves. Open radiation boundary condition is imposed at the east end of the channel to allow the waves to pass out without reflection. The initial source of maximum height of 1 m is chosen to be located at X, with a vertical distribution represented by a Gaussian hump given by $\eta = ae^{-(x_x^{\sigma})^2}e^{-(y_y^{\sigma})^2}$ with standard deviations σ_x of 1500 m and σ_y of 2500 m (Fig. 2). A grid size of 50 m and a time step of 1.25 s are used. Several observation points are placed in the study domain to record the simulated time series for the comparisons between TUNA and COMCOT. The results simulated by TUNA compare well with the results simulated by COMCOT as shown in Figs. 3 and 4, indicating proper performance of TUNA. Fig. 3 shows the comparison between TUNA (left) and COMCOT (right) simulated time series for wave heights at three selected locations (the remaining locations not shown). Fig. 4 depicts snapshots simulated by TUNA (left) and COMCOT (right) at several time intervals. Several other comparisons between TUNA and COMCOT

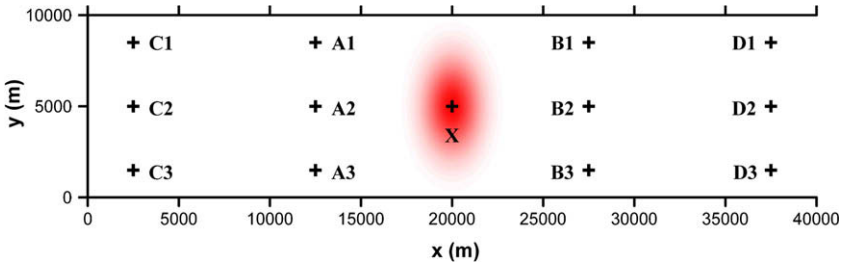

Fig. 2. Computational domain with observation points and initial Gaussian hump.

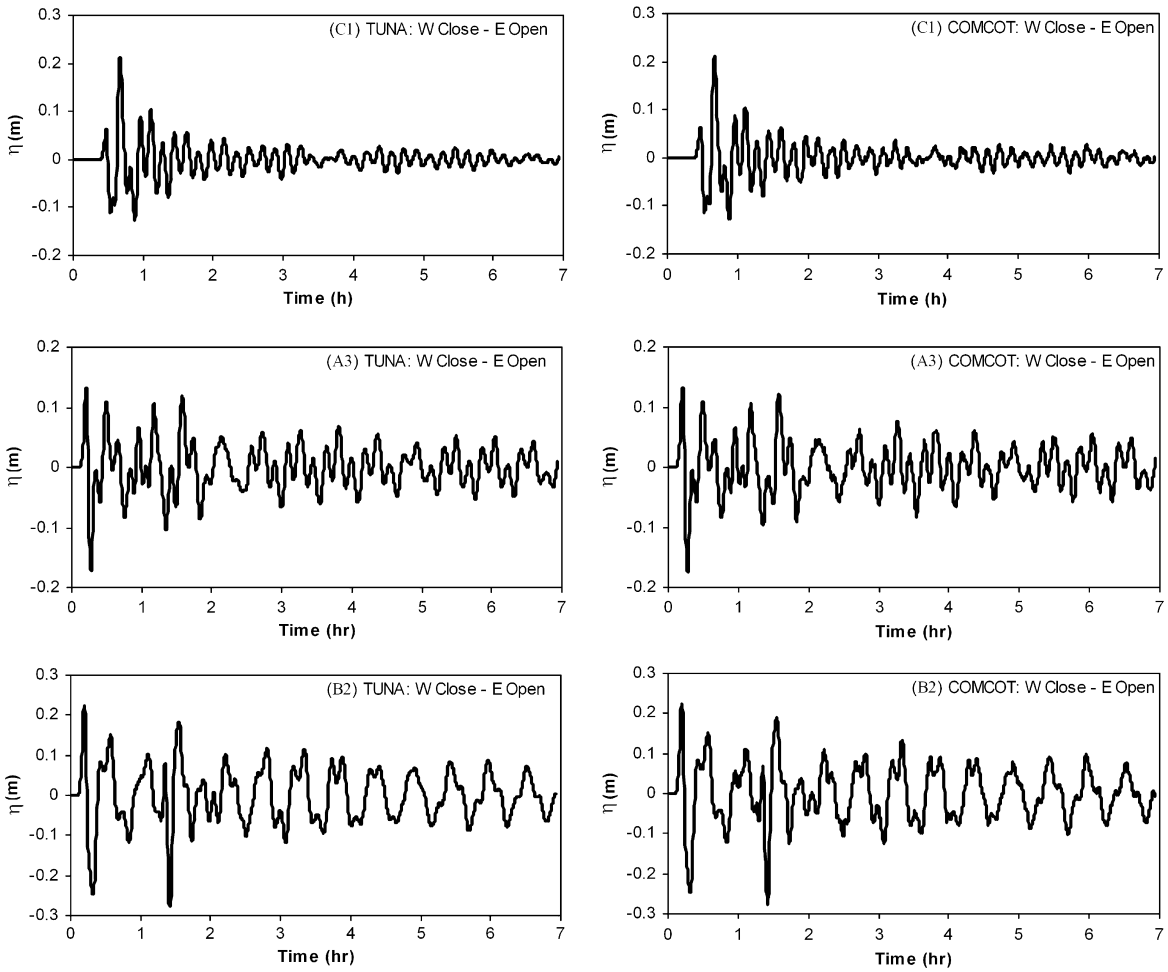

Fig. 3. Wave height time series at 3 locations to compare TUNA (left) and COMCOT (right).

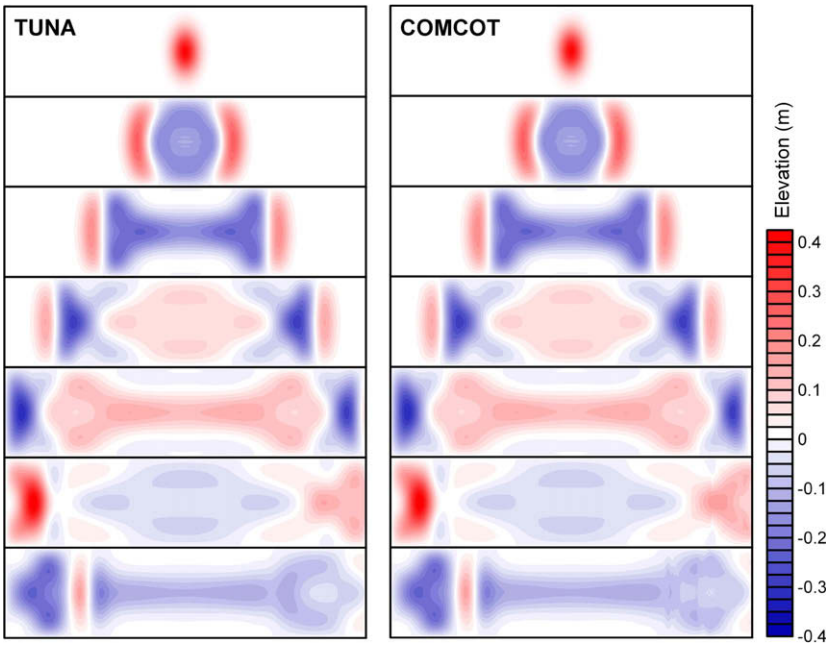

Fig. 4. Wave height snapshots at 7 time steps to compare TUNA (left) and COMCOT (right).

were also performed, indicating good agreements between the two models. Hence we may now use TUNA with confidence regarding its performance and credibility.

4. 26 December 2004 tsunami propagation

In this paper we are concerned about the risks of tsunami originating from the Andaman sea regions on the northwest coast of Peninsular Malaysia, including Penang and Langkawi. The choice of the study areas is based upon the perceived vulnerability of these areas from future tsunamis. The chosen computational domain of dimension 1500 km by 1200 km containing these areas is shown in Fig. 5. As regards the source terms, there are various estimates for the source dimensions for the 26 December 2004 tsunami reported in the literature (Ammon et al., 2005; Annunziato and Best, 2005; ASCE, 2005; Cheesman et al., 2005; DCRC, 2005; Harinarayana and Hirata, 2005; Lay et al., 2005). Table 1 provides a summary of these initial tsunami generation sources. It is generally accepted that the runup height in the near field would not exceed twice the fault slip/height. Stein and Okal (2005) had earlier estimated a tsunami source dimension of about 1200 km × 200 km × 11 m (length × width × slip). However, the measured tsunami runup height of about 25 m to 30 m reported in the near-field around Sumatra (Borrero, 2005) would imply that the fault slip might be more than 11 m, possibly between 12–15 m. Hence Okal and Stein (2005) suggested an alternative source dimension of 1200 km × 200 km × 13 m. However, DCRC (2005) preferred a source dimension of 800 km × 85 km × 11 m. It has also been reported that the most significant tsunami waves were generated indeed by a source of a length of about 600 km–800 km located along the southern portion of the entire range of initial disturbances or eruptions (Lay et al., 2005; Xu and Chen, 2005). The source generation terms used in this paper is generated by considering the entire range of source disturbances of 1200 km by 200 km. Based upon simulation results as well as simple arguments, the northern most portion of the initial source disturbance would not contribute much towards generating tsunamis onto Malaysian coasts. These northern generating sources contribute significant tsunami waves onto northern Thailand however. These initial source disturbances are implemented in two ways as follows.

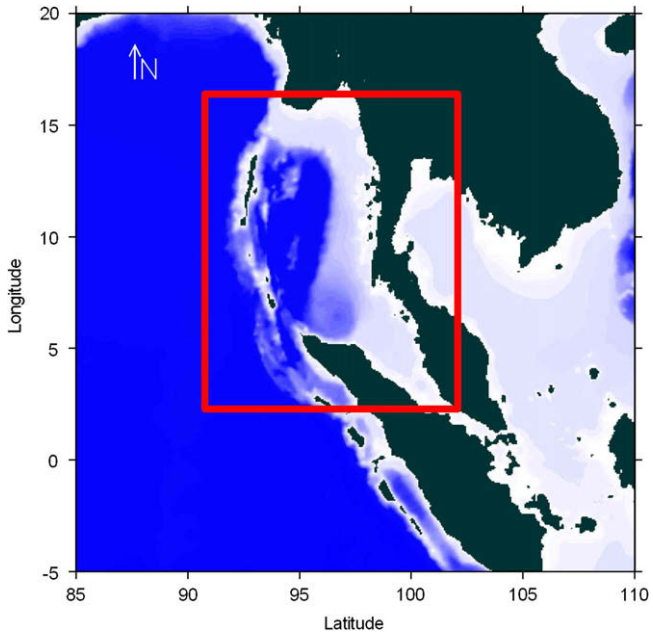

Fig. 5. Map of study area with computational domain shown in rectangle.

5. Source generation terms

5.1. Simple Gaussian Hump

The source generation term used in this section is derived from extensive literature review relating to the 26 December 2004 Andaman tsunami as listed in Table 1. The initial source of tsunamis will be generated in two ways. We first evaluate the appropriate-

Table 1
Andaman tsunami source dimension obtained from literature.

Source size			Reference	Comment
Length (km)	Width (km)	Displacement (m) (average)		
900	100	15	Annunziato and Best (2005) and Cheesman et al. (2005)	Assumed by S. Ward
800	85	11	DCRC (2005), Harinarayana and Hirata (2005)	
700	100	20	Annunziato and Best (2005)	Used by Istituto Nazionale Geofisica e Vulcanologia (INGV)
1200	200	13	Okal and Stein (2005)	
1300	150	20	ASCE (2005);Stein and Okal (2005)	
420	240	5–20 (7)	Lay et al. (2005)	Sumatra segment
325	170	(5)		Nicobar segment
570	160	<2		Andaman segment
200	150	20	Annunziato and Best (2005)	Sumatra segment
670	150	20		Nicobar segment
300	150	20		Andaman segment
446	170	13.7 (+ve) 8.6 (−ve)	Yalciner et al. (2005a)	
443	170	10.7 (+ve) 6.6 (−ve)	Yalciner et al. (2005b)	
1200–1300	150	15 (peak)	Ammon et al. (2005)	
1300	150	20	ASCE (2005)	

ness of a source term in the form of a simple Gaussian hump shape (Yoon, 2002). This chosen source has the estimated dimension of 1200 km × 200 km × 12 m as reported in the literature. The source term, in one dimension, would consist of an initial vertical displacement given by a Gaussian hump formula $\eta = ae^{-(x_x^\sigma)^2}$. In two dimensions it is given by $\eta = ae^{-(x_x^\sigma)^2} e^{-(y_y^\sigma)^2}$. Hence in this paper we initially chose a Gaussian form consisting of $a = 12.0$ m, $\sigma_x = 100$ km, $\sigma_y = 600$ km to approximate the chosen source. However, this choice of dimension would imply a larger source domain. Hence we subsequently decided to use $a = 12.0$ m, $\sigma_x = 60$ km, $\sigma_y = 450$ km instead in order to better approximate the chosen initial source of 1200 km × 200 km × 12 m. Slight variations about this chosen source dimension would not have significant impacts on the simulation results on Malaysia. The resulting initial Gaussian hump source used in this paper is shown in Fig. 6.

5.2. Okada source term

A second form of initial source of tsunami may be generated by means of the Okada formulation. The input parameters for the Okada source term used in this study are derived from literature search with slight adaptation to better estimate reported values. They consist of the following parameters: fault length = 1000 km, fault width = 100 km, dip angle = 8°, slip angle = 110°, strike angle = 350°, focal depth = 30000 m and displacement = 20 m (Rao, 2007; Mishra and Rajasekhar, 2005). Details regarding the formulation of the Okada model can be referred to Okada (1985). The resulting source simulated by TUNA using the Okada model is shown in Fig. 7, indicating a leading depression *N* wave. This initial tsunami source is in close agreement with that generated by COMCOT, using the formulation of Masinha and Smylie (1971).

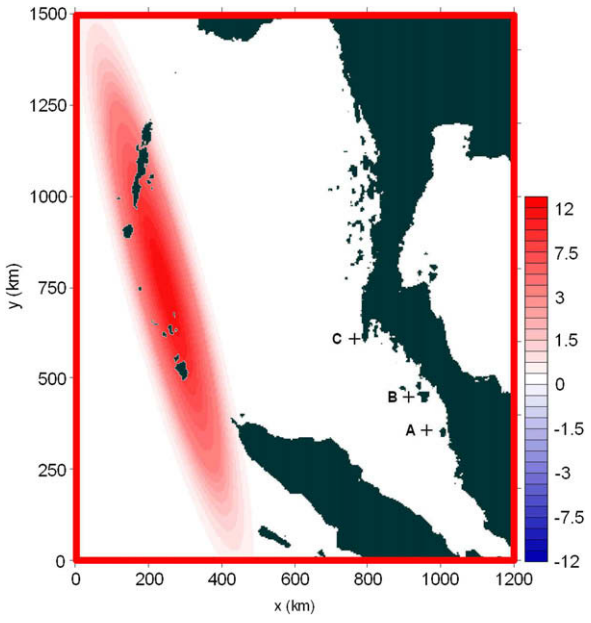

Fig. 6. Initial Gaussian hump tsunami source.

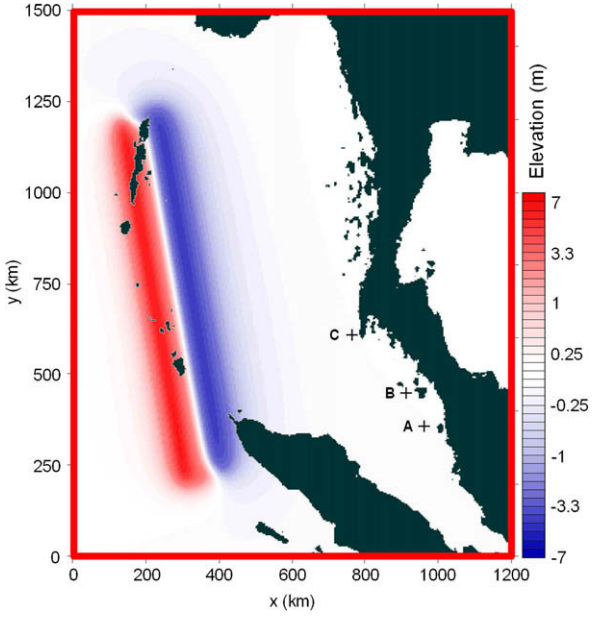

Fig. 7. Initial Okada tsunami source.

6. Propagation of tsunami

6.1. Propagation of simple Gaussian hump

The initial tsunami source term in the form of a simple Gaussian hump as shown in Fig. 6 in Section 5.1 is now used to simulate tsunami propagation towards the coasts of Malaysia by means of tsunami propagation model TUNA-M2. For the first initial simulation, we opted for a coarse bathymetry approximated from Admiralty Charts (1366, 3944 and 4706) and simple interpolation to provide an initial desktop simulation as a start. We wish to investigate the importance of good bathymetry and good initial source term on the accuracy of simulated tsunami arrival time and off shore wave heights and shape. Solid reflective boundary condition is imposed on all sea–land boundaries so as to act as a reflective surface. The computational grid size is 1000 m, resulting in a total of 1.8 million nodes. The time step used is 1 s, although 3 s are adequate. The simulated results summarized in the form of snapshots are displayed in Fig. 8 at intervals of 1000 s. The initial source term splits into two halves, one propagating towards Malaysia, while the other towards the west into the Indian Ocean. The waves first arrive at Phuket (location C in Fig. 6) after about one hour. This arrival time appears to be too early as compared to eyewitness account (UKM, 2006). A careful analysis confirms that this discrepancy is due to the coarse bathymetry used, which resulted in simulation depths that are significantly deeper than the actual depths. The simulated arrival times for Penang (location A) and Langkawi (location B) are also too early for similar reasons. The time series of wave heights at three selected observation locations are plotted in Fig. 9, indicating leading elevation *N* waves, which contradict eyewitness accounts. Field surveys conducted in Malaysia recorded observations of an initial sudden depression or withdrawal of sea levels before the onslaught of the subsequent elevation, indicating a leading depression *N* wave. Hence this initial generating tsunami source in the form of a simple Gaussian hump is not appropriate for the 26 December 2004 Andaman tsunami. An appropriate initial source should be a leading depression *N* wave. Further the bathymetry used should be improved by using ETOPO5 bathymetry. These two improvements will be implemented in the next section.

6.2. Propagation of Okada source

To provide improved simulations we now choose the initial source generating term by adopting the Okada formulation with parameter values as cited in Section 5.2, derived from the literature, to replace the simplified Gaussian hump shape used earlier. We hope to obtain a leading depression *N* wave for the initial

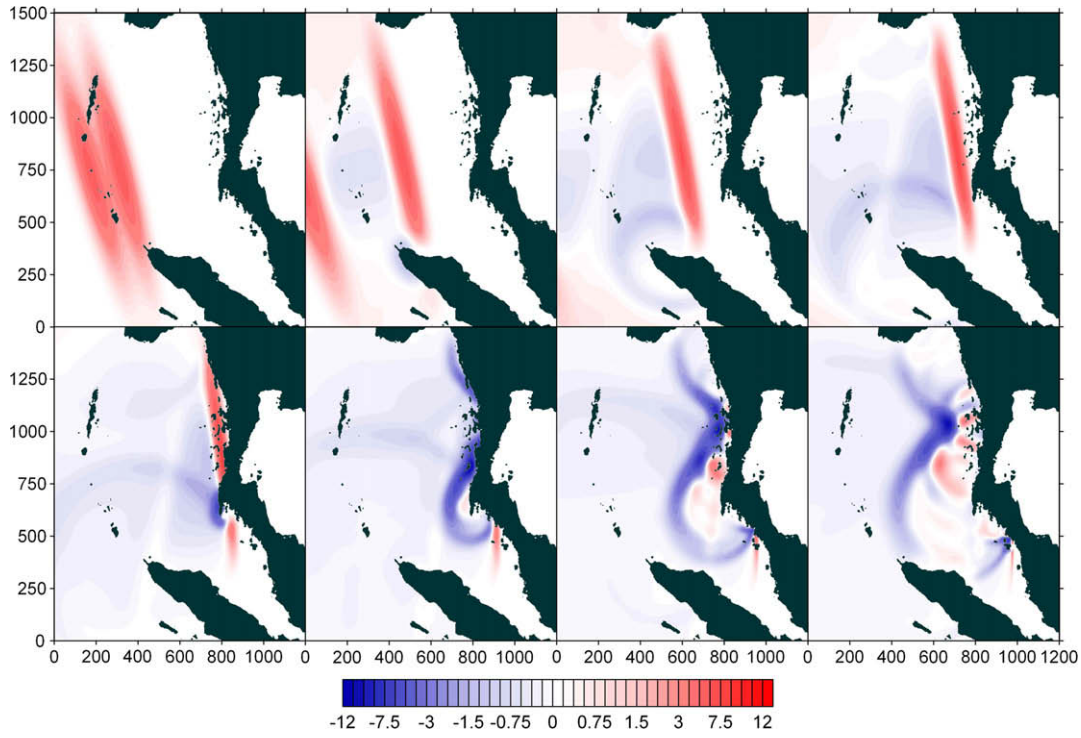

Fig. 8. Tsunami propagation snapshots due to initial Gaussian hump source.

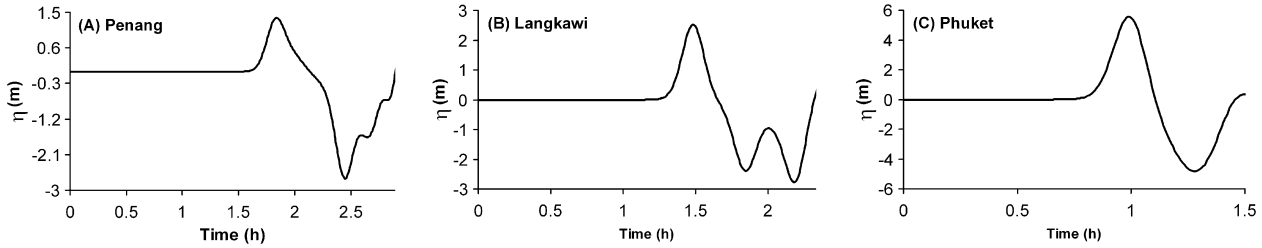

Fig. 9. Time series of tsunami propagation due to initial Gaussian hump source.

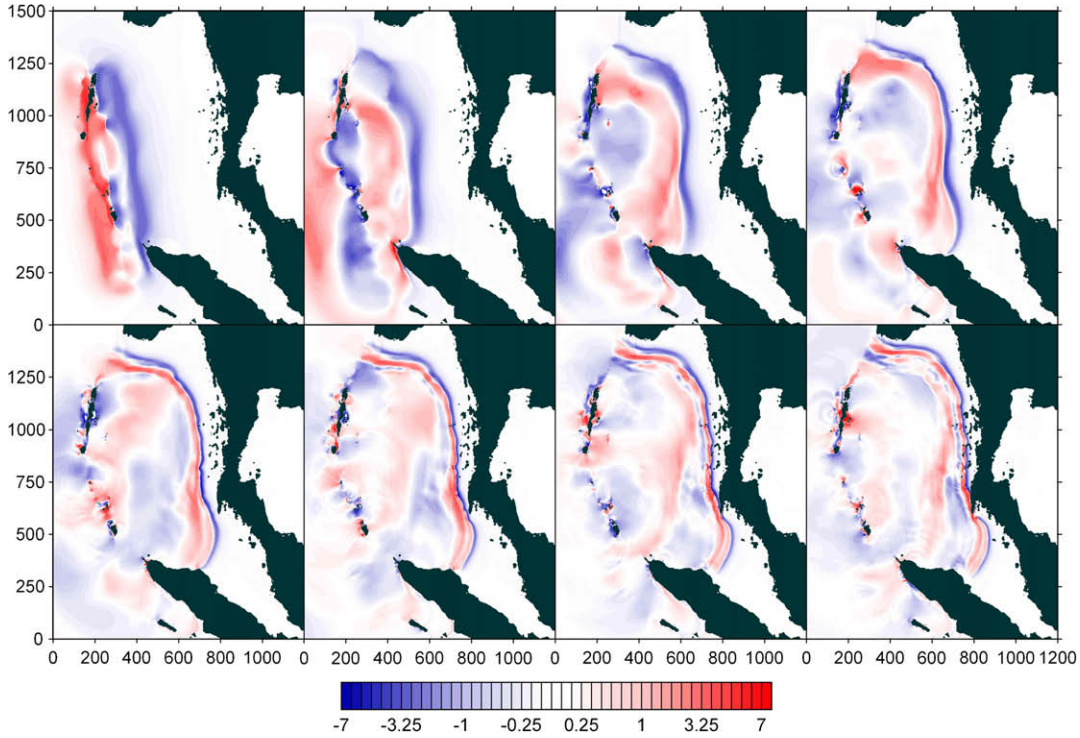

Fig. 10. Tsunami propagation snapshots due to initial Okada source.

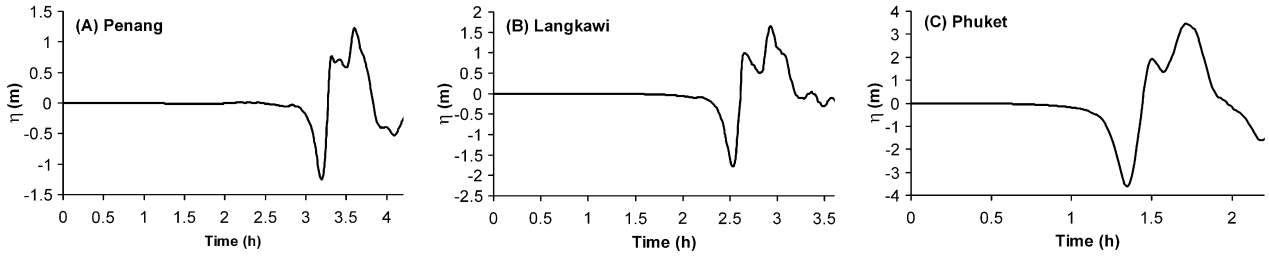

Fig. 11. Time series of tsunami propagation due to initial Okada source.

source in order to match eyewitness account of the initial waveform indicating a leading depression *N* wave. We use ETOPO5 with linear interpolation to improve on bathymetry. The same grid size of 1000 m and time step of 1 s are used, resulting in a total of 1.8 million nodes. The initial source generating the tsunami is depicted in Fig. 7, indicating a leading depression *N* wave as desired. The simulation results summarized in a series of snapshots at intervals of 1000 s are illustrated in Fig. 10. The initial leading depression *N* waves propagate eastwards towards Thailand and Malaysia, whilst the initial leading elevation *N* waves propagate westwards. The first waves arrive offshore of Phuket after 1.8 h, following a leading depression. The simulated waves arrive at Langkawi after 3 h and at Penang after 3.6 h, following a leading depression for both places. These simulated results agree with eyewitness account, both in terms of arrival times as well as the shape of the waves in the form of leading depression *N* waves (UKM, 2006). Two slightly different arrival times are reported based upon field interviews and observations by the study team and UKM (2006). The arrival times at Penang are 13:10–13:15 for the first waves and 13:15–13:30 for the second waves. For Langkawi, the arrival times are 12:35–12:40 and 12:40–13:00 for the first and second waves respectively. However the arrival times for the third waves cannot be reliably estimated. The earthquake that triggered the tsunami occurred at 00:58:53 UTC (08:58:53 Malaysian time). The simulated wave height time series at the three selected observation locations are demonstrated in Fig. 11. The simulated maximum wave heights offshore at depths of 50 m are 3.6 m, 1.5 m and 1.2 m at Phuket, Langkawi and Penang, respectively. These maximum wave heights agree qualitatively with surveyed runup heights along beaches in Phuket, Langkawi and Penang, taking into account amplification of wave offshore by a factor of up to three along the shallow beaches (Teh et al., 2008).

7. Post tsunami surveys

Post tsunami surveys were conducted twice in 2005 along tsunami-impacted beaches in Peninsular Malaysia by the authors in collaboration with a team of tsunami experts from Korea. Fig 12 shows the map of Peninsular Malaysia, including the four worst impacted areas namely Penang, Langkawi, Kedah and Perak. The location numbers refer to those listed in Table 2, which also provides a summary of runup heights and inundation distances. The surveyed tsunami runup heights along the beaches in Penang vary between 2.3 m and 4.0 m, while those in Langkawi are between 2.2 m and 3.7 m. For the state of Kedah excluding Langkawi the runup heights were observed to vary between 0.38 m and 3.8 m

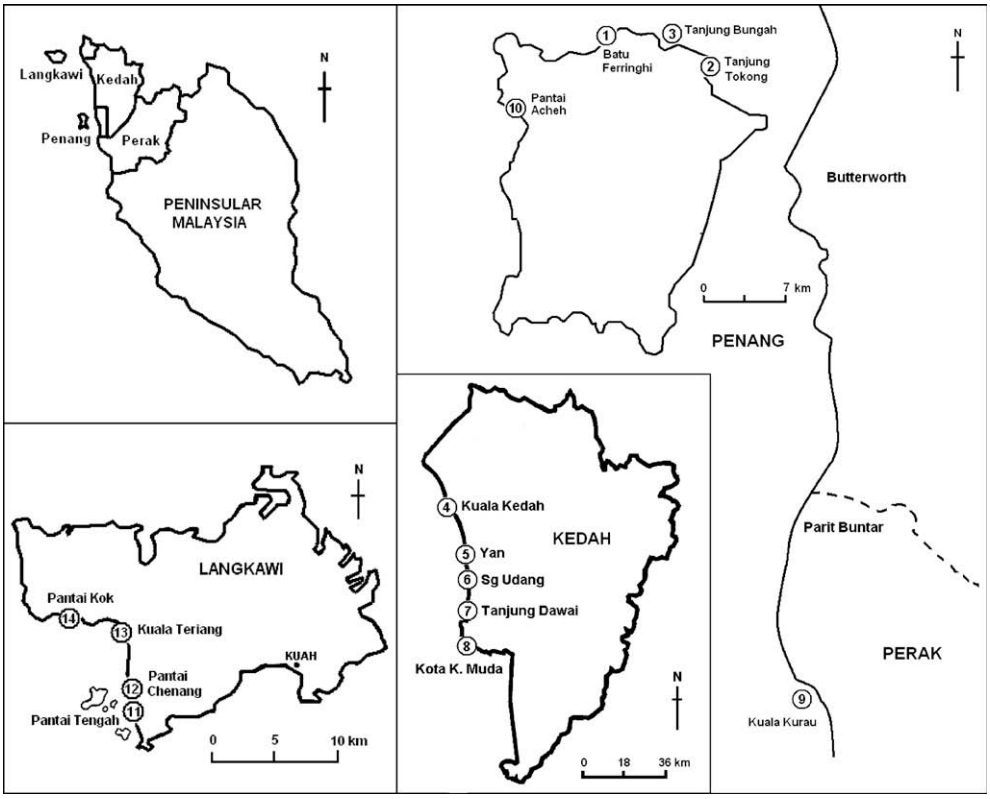

Fig. 12. Map of Malaysia, including Penang and Langkawi, showing impacted areas.

Table 2
Survey runup heights for the December 26 2004 tsunami.

	Location Name	Date (2005)	Latitude (N)		Longitude (E)		Runup height (m)	Inundation distance (m)
			Deg.	Min.	Deg.	Min.		
1a	B. Ferringhi (Teluk Bayu)	20 Apr.	5	28.26	100	14.63	3.460	19.200
1b	B. Ferringhi (Miami Beach)	20 Apr.	5	28.67	100	16.07	4.000	25.600
2a	Tanjung Tokong	20 Apr.	5	27.62	100	18.48	3.650	35.800
2b	Tanjung Tokong	20 Apr.	5	27.57	100	18.41	N/A	190.000
2c	Tanjung Tokong	20 Apr.	5	27.70	100	18.50	2.610	18.300
3a	Tanjung Bungah	21 Apr.	5	28.21	100	16.66	2.310	18.380
3b	Tanjung Bungah	21 Apr.	5	28.20	100	16.65	2.940	36.200
4	Kuala Kedah	22 Aug.	6	6.00	100	26.00	0.900	N/A
5	Yan (Kg. K.S. Limau)	22 Aug.	5	53.00	100	21.00	1.227	12.900
6	Sg udang	22 Aug.	5	48.00	100	22.00	1.500	N/A
7	Tanjung Dawai	22 Aug.	5	40.00	100	21.00	0.385	75.319
8	Kota K. Muda	22 Aug.	5	34.00	100	20.00	3.800	100.524
9	Kuala Kurau	23 Aug.	5	0.00	100	25.00	1.930	N/A
10	Pantai Acheh	23 Aug.	5	24.00	100	11.00	2.505	13.400
11	Pantai Tengah (Lanai Hotel)	24 Aug.	6	15.00	99	43.00	3.660	44.500
12	Pantai Chenang (Pelangi Hotel)	24 Aug.	6	17.00	99	43.00	3.749	54.720
13	Kuala Teriang	24 Aug.	6	21.00	99	42.00	3.091	27.038
14a	Pantai Kok (Mutiara Beach Resort)	24 Aug.	6	21.00	99	40.00	2.246	50.840
14b	Pantai Kok (Berjaya Hotel)	24 Aug.	6	21.00	99	40.00	2.983	34.879

exhibiting significant scattering. These variations in runup wave heights have also been reported in the literature, the reasons for which vary. However, local features such as bathymetry, land curvature and sea–land nonlinear interactions are among the most significant causes of these variations in runup wave heights. Detailed information regarding local bathymetry, beach topography and sea–land nonlinear wave interactions are necessary in order to better understand these local variations in runup wave heights. For example the presumed solid boundary condition prescribing total reflection of wave on land boundary will not be appropriate for beach runup simulation. For this purpose moving boundary conditions applied to NWSE with small grid size are more appropriate, for which a separate component TUNA-RP has been developed. For Penang a series of simulations by TUNA-RP, with grid size of 5 m, have indicated that a tsunami wave of 1.2 m arriving off shore at a depth of about 50 m in Penang (simulated by TUNA-M2) may be amplified to 2.4 m to 3.6 m, depending on beach roughness, slope and length, indicating an amplification factor of 2–3. This simulated runup wave heights agree qualitatively with observed maximum wave heights reported. The scattering

of data notwithstanding, these post survey results for Penang have provided some measure of verification of simulated tsunami propagation wave heights computed by TUNA. For Langkawi, simulation by TUNA-M2 followed by TUNA-RP would have resulted in maximum beach runup heights of 4.5 m, which is a slight over prediction as compared to surveyed maximum runup heights of 3.8 m. It has been suggested that the wave breakers located off shore of Langkawi might have provided some mitigation effect by reducing incoming tsunami wave heights. This tentative observation has provided the incentive to investigate the role of tsunami mitigation played by coastal structures, vegetation and mangrove, the results of which will be reported in a separate paper in this issue.

The authors have focused on the numerical simulation of tsunami as an integral component of a national program to mitigate the adverse impact of future tsunamis in Malaysia. Other research groups devote their attentions to data collection and issues related to the environmental, socio-economic and community well being (UKM, 2006). Instrumentation essential to enable the ability to provide and confirm early warning regarding the arrival of potentially destructive tsunamis must be and have been put in place (MMS, 2007). It is hoped that this integrated approach would help develop and enable coastal communities to be more tsunami resilient.

8. Conclusion

In conclusion the following observations may be made. Based upon documented eyewitness accounts, the observed tsunami waves in Penang and northwest Peninsular Malaysia conform to leading depressions *N* waves. These leading depressions *N* waves can be generated by the Okada model, but not by the simplified single Gaussian hump. Good bathymetry is essential for a proper simulation of tsunami propagation, particularly with respect to wave arrival times, since the wave celerity is proportional to the square root of water depth. The bathymetry with grid size of 1000 m used in this study is interpolated from ETOPO5. This resolution is adequate to represent the bathymetry in the deep ocean, where the wavelengths are typically long of the order of 100 km. Further in the deep ocean, friction is insignificant due to its depth; hence friction may be omitted optionally in TUNA-M2. However, for the simulation of beach runup by TUNA-RP, friction and nonlinearity are important and must be incorporated with a moving boundary algorithm to be implemented with small grid size of 10 m or less, due to the existence of waves with short wavelengths. Post tsunami surveys conducted by the authors as well as by others provide some data regarding runup heights and tsunami arrival times along beaches in Penang and Langkawi. The scattering of beach runup heights notwithstanding, these survey data provide some degree of calibration and validation of TUNA and COMCOT. In general we are confident that in some aspects TUNA is as capable as other tsunami simulation models such as COMCOT since both models appear to provide similar results. The risk of future tsunamis impacting on northwest Peninsular Malaysia remains a real concern, due to continuing seismic activities in the Andaman regions. Yet the science of earthquakes and tsunami prediction is still in the infancy. Much research is urgently needed to improve the science and arts of tsunami predictions.

Acknowledgement

Financial support provided by Grants #305/PMATHS/613131, #1001/PPTM/817006 and #1001/PMATHS/817025 are gratefully acknowledged.

References

Ammon, C.J., Ji, C., Thio, H.K., Robinson, D., Ni, S., Hjorleifsdottir, V., Kanamori, H., Lay, T., Das, S., Helmberger, D., Ichinose, G., Polet, J., Wald, D., 2005. Rupture process of the 2004 Sumatra–Andaman earthquake. Science, 308, 1133–1139.

Annunziato, A., Best, C., 2005. The Tsunami Event Analyses and Models. Institute for the Protection and Security of the Citizen, Joint Research Centre, European Commission.

ASCE, 2005. Sumatra–Andaman Islands earthquake and tsunami of December 26, 2004 lifeline performance. In: Carl Strand and John Masek (Eds.), Technical Council on Lifeline Earthquake Engineering, Monograph No. 29, American Society of Civil Engineers, p. 271.

Borrero, J.C., 2005. Field survey of northern Sumatra and Banda Aceh, Indonesia after the tsunami and earthquake of 26 December 2004. Seismol. Res. Lett. 75 (3), 312–320.

Cheesman, P., Hall, N., Day, S., 2005. The Asian Earthquake/Tsunami Disaster: An Insurance Perspective. Glencairn Limited.

Disaster Control Research Center (DCRC), 2005. Modeling a Tsunami Generated by Northern Sumatra Earthquake [12/26/2004]. Tsunami Engineering Laboratory, Disaster Control Research Center, Tohoku University, Japan.

Harinarayana, T., Hirata, N., 2005. Destructive earthquake and disastrous tsunami in the Indian Ocean, What next? special correspondence. International association for- Gondwana research, Japan. Gondwana Res. (Gondwana Newsletter Section) 8(2), 246–257.

Hérbert, H., Schindelé, F., Altinok, Y., Alpar, B., Gazioglu, C., 2005. Tsunami hazard in the Marmara sea (Turkey): a numerical approach to discuss active faulting and impact on the Istanbul coastal areas. Mar. Geol. 215, 23–43.

Imamura, F., Shuto, N., Goto, C., 1988. Numerical simulation of the transoceanic propagation of tsunamis. In: Proceedings of Paper presented at the Sixth Congress of the Asian and Pacific Regional Division, Int. Assoc. Hydraul. Res., Kyoto, Japan.

Intergovernmental Oceanographic Commission (IOC), 1997. Numerical method of tsunami simulation with the leap frog scheme, 1, shallow water theory and its difference scheme. In: Manuals and Guides of the IOC, Intergovernmental Oceanogr. Comm., UNESCO, Paris (pp. 12–19).

Koh, H.L., Teh, S.Y., Izani, A.M.I., 2007. Tsunami Mitigation Management Technology, Asia Pacific Tech Monitor, Nov–Dec 2007 24 (6) Special Features, pp 47–54, The United Nations Asian and Pacific Centre for Transfer of Technology (UN-APCTT), India.

Koh, H.L., Teh, S.Y., Izani, A.M.I., 2005. Meso scale simulation of December 26 2004 tsunami with reference to Malaysia and Thailand. In: Proceedings of Third International Symposium on Southeast Asian Water Environment, 6–8 December 2005, The University of Tokyo and Asian Institute of Technology (AIT), Bangkok, Thailand, pp 89–96.

Lay, T., Kanamori, H., Ammon, C.J., Nettles, M., Ward, S.N., Aster, R.C., Beck, S.L., Bilek, S.L., Brudzinski, M.R., Butler, R., DeShon, H.R., Ekström, E, Satake, E., Sipkin, S., 2005. The great Sumatra–Andaman earthquake of 26 December 2004. Science 308, 1127–1133.

Liu, P.L.-F., Woo, S.B., Cho, Y.S., 1998. Computer Programs for Tsunami Propagation and Inundation, Cornell University, Sponsored by National Science Foundation (p. 104).

Masinha, L., Smylie, D.E., 1971. The displacement fields of inclined faults. B. Seismol. Soc. Am. 61 (5), 1433–1440.

Mishra, D.C., Rajasekhar, R.P., 2005. Tsunami of 26 December 2004 and related tectonic setting. Curr. Sci. India 88 (5), 680–682.

MMS, 2007. NATIONAL REPORT: Submitted by MALAYSIA, Presented by Malaysian Meteorological services (MMS) in ICG/PTWS-XXII, 17–20 September 2007, Guayaquil, Ecuador, p. 14 www.inocar.mil.ec/webpages/PTWS/docs/National_Reports/PTWS-XXII_Malaysia_National_Report_public.pdf.

Okada, Y., 1985. Surface deformation due to shear and tensile faults in a half-space. B. Seismol. Soc. Am 75 (4), 1135–1154.

Okal, E.A., Stein, S., 2005. Ultra-long period seismic moment of the Sumatra earthquake: implications for the slip process and tsunami generation, Eos Trans. American Geophysical Union (AGU) 86 (18), Jt. Assem. Suppl., Abstract U43A-02, Meetings 2005 Joint Assembly. 23–27 May 2005, New Orleans, Louisiana, USA.

Rao, N.P., 2007. Characterization of Potential Tsunamigenic Earthquake Source Zones in the Indian Ocean. Tsunami and Nonlinear Waves Part II. Springer Berlin Heidelberg (pp. 285–312).

Stein, S., Okal, E., 2005. Long Period Seismic Moment of the 2004 Sumatra Earthquake and Implications for the Slip Process and Tsunami Generation. Northwestern University.

Teh, S.Y., Koh, H.L., Izani, A.M.I., 2006. A model investigation on tsunami propagation in Malaysian and Thailand coastal water, association of engineering education in southeast and east Asia and the Pacific (AEESEAP). J. Eng. Edu. 31, 7–14.

Teh, S.Y., Koh, H.L., Izani, A.M.I., Lee, H.L. 2008. Modeling tsunami runup by moving boundary. In: Proceedings of the Symposium on Giant Earthquakes and Tsunamis, 22–24 January 2008, The University of Tokyo, Phuket, Thailand, pp. 301–306.

Titov, V.V., Synolakis, C.E., 1997. Extreme inundation flows during the Hokkaido-Nansei-Oki tsunami. Geophys. Res. Lett. 24 (11), 1315–1318.

Universiti Kebangsaan Malaysia (UKM), 2006. The 26.12.04 tsunami disaster in Malaysia: an environmental, socio-economic and community well-being

impact study. In: Ibrahim Komoo and Mazlan Othman (Eds.), Institut Alam Sekitar dan Pembangunan (LESTARI) and Akademi Sains Malaysia, p. 168.

Xu, L.S. and Chen, Y.T., 2005. Source process of the 2004 Sumatra-Andaman Mw9.0 earthquake. In: Chen Yun-tai (Ed.), Proceedings Volume of the Asia-Oceania Geosciences Society (AOGS) 2nd Annual Meeting 2005 in Singapore, 20–24 June 2005.

Yalciner, A.C., Pelinovsky, E.N., Kuran, U., Taymaz, T., Zaitsev, A., Ozyurt, G., Ozer, C., Karakus, H., Safak, I., 2005a. Simulation and Comparison with Field Survey Results of Dec., 26, 2004 Tsunami.

Yalciner, A.C., Perincex, D., Ersoy, S., Presateya, S., Hidayat, R., McAdoo, B., 2005b. Report on 26 December 2004 Indian Ocean tsunami, Field survey during 21–31 January, North of Sumatra by ITST, UNESCO IOC.

Yoon, S.B., 2002. Propagation of distant tsunamis over slowly varying topography. J. Geophys. Res 107 (C10), Am. Geophys. Union (pp. 4.1–4.11).